Supplement of Geosci. Model Dev., 17, 5545–5571, 2024
https://doi.org/10.5194/gmd-17-5545-2024-supplement

Geoscientific Model Development
Open Access
EGU

Supplement of

Evaluating CHASER V4.0 global formaldehyde (HCHO) simulations using satellite, aircraft, and ground-based remote-sensing observations

Kengo Sudo et al.

Correspondence to: Hossain Mohammed Syedul Hoque (hoquesyedul@gmail.com, hoque.hossain.mohammed.syedul.u6@f.mail.nagoya-u.ac.jp)

S1. Impact of model resolution and other model error sources.

The coarse horizontal and vertical resolution can lead to additional errors related to atmospheric transport and chemical processes. Seasonal variations in the HCHO levels in different regions, simulated at 1.4˚ × 1.4˚ resolution, are compared with the standard simulations in Fig S1. The statistics are listed in Table S1.

Except for the Indian regions, both simulations' absolute values are similar. The MBE between the two simulations over the Indian regions (IGP, S-India, and N-India) is ~ 2 × 10^{15} molecules cm^{-2}. Over E-India and S-India, the MBE between the standard simulation TROPOMI observations is ~1.5 × 10^{15}molecules cm^{-2}. This signifies that high-resolution simulations will reduce the model-observation MBE in these regions by at least ~25%.
Chemical kinetics described in the model can also induce uncertainties. The simulations do not consider direct emissions of HCHO from anthropogenic and pyrogenic sources. Photolysis of glyoxal, the most abundant di-carbonyl in the atmosphere, is a crucial HCHO production pathway (Vrekoussis et al., 2010). The current CHASER VOC scheme doesn't include glyoxal reactions and byproducts. Simulations with updated VOC chemistry schemes and emission inventories will be addressed in detail in a separate article.

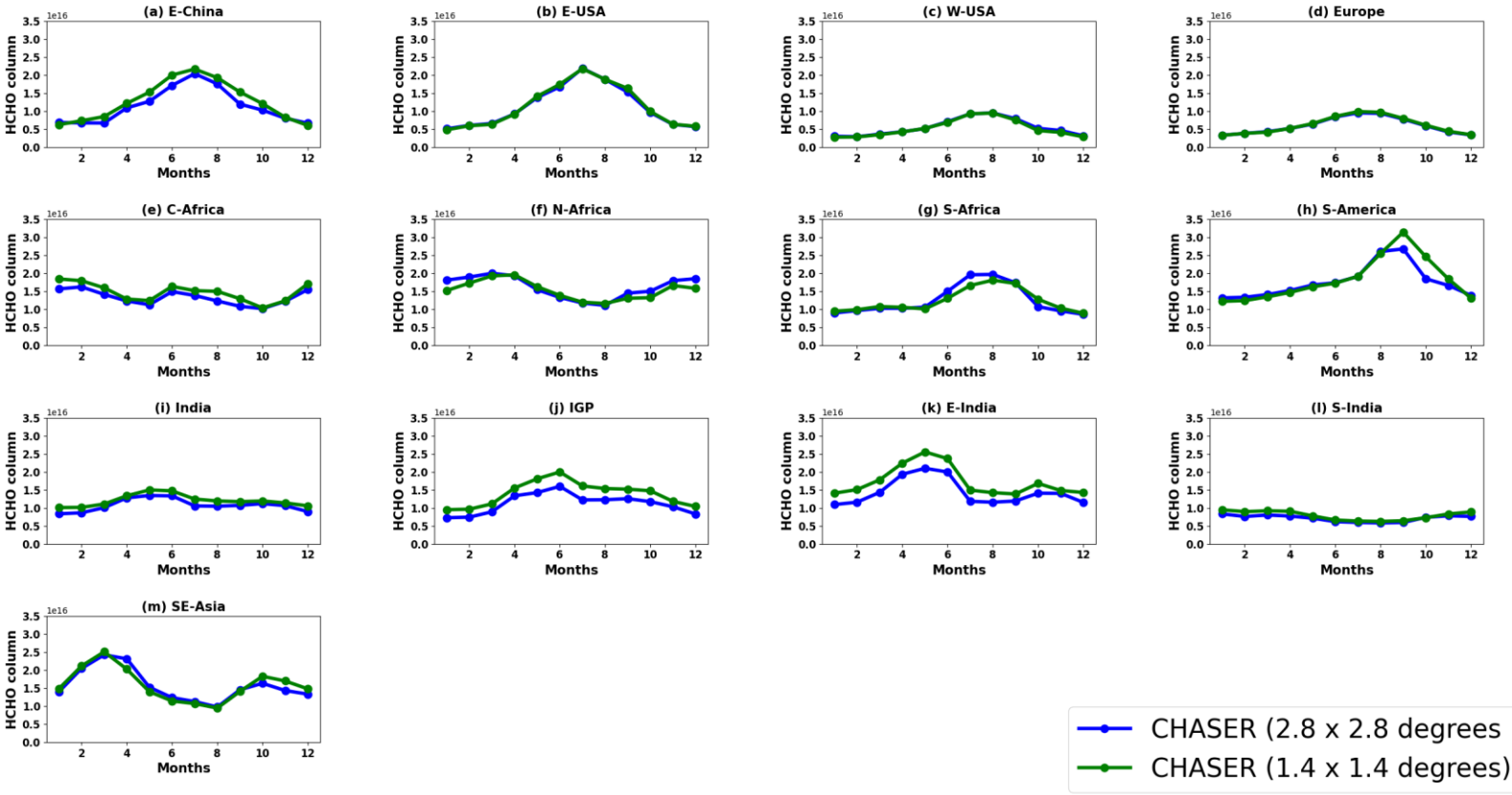

Figure S1. Monthly variations in HCHO columns in the selected regions, simulated at 2.8˚× 2.8˚ (blue, standard simulation) and 1.4˚ × 1.4˚ resolutions (green, high resolution). The coordinate bounds are similar to Fig.2.

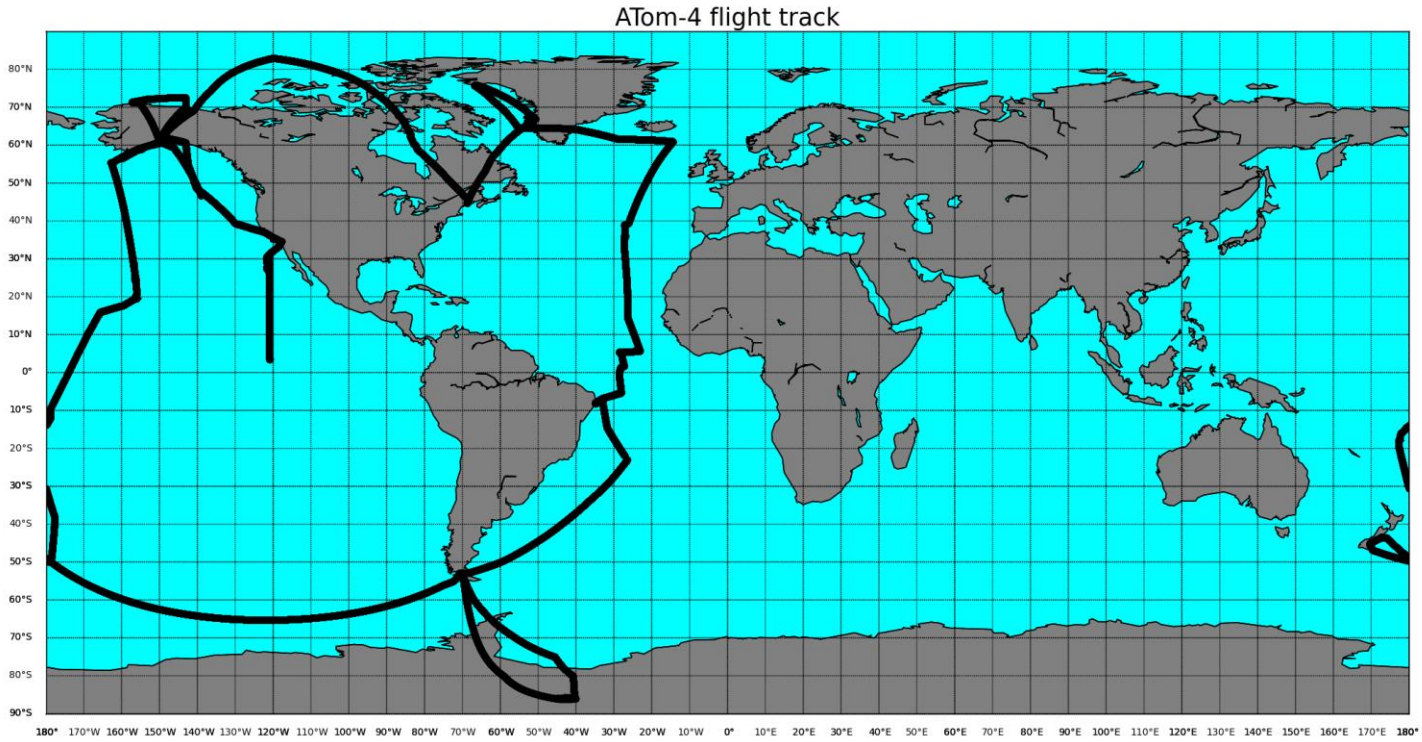

Figure S2. Atom-4 flight track.

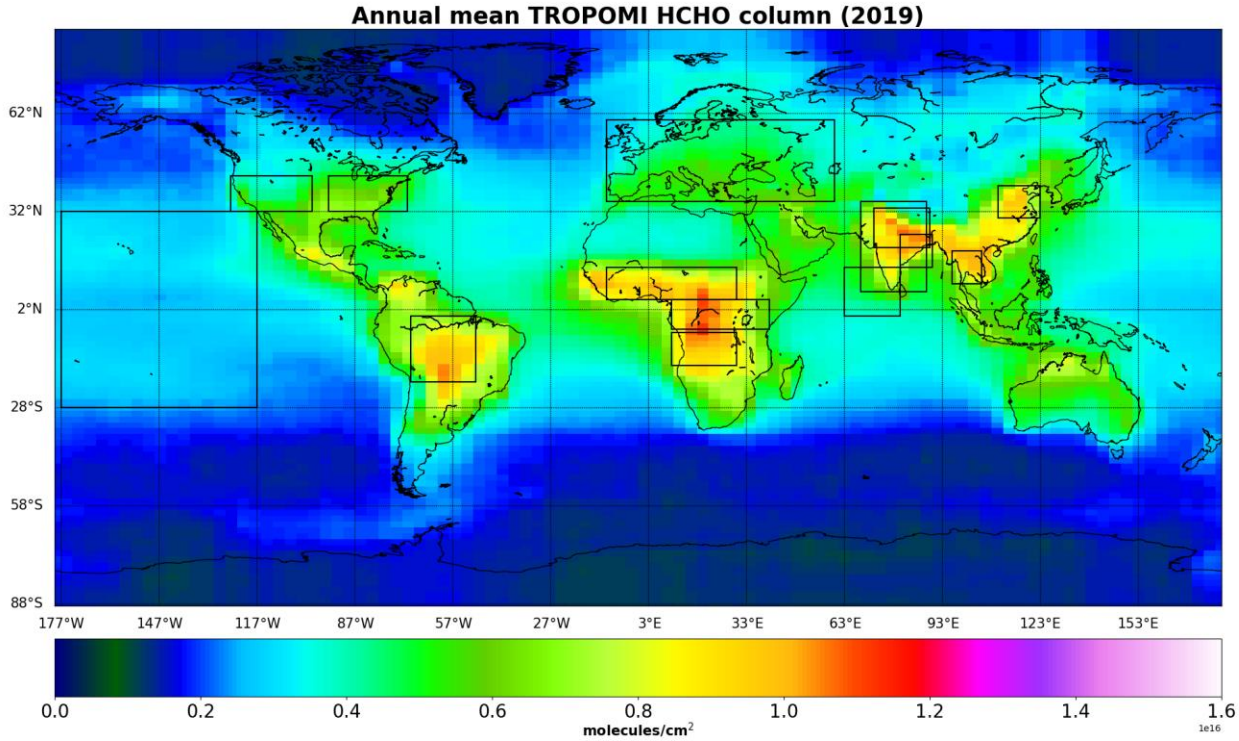

Figure S3. The global annual mean TROPOMI HCHO columns were calculated from the observation in 2019. The black boxes indicate the regions of interest discussed in the results and discussion section. The coordinate bounds of the regions are as follows: Eastern China (E-China; 30–40°N, 110–123°E), eastern United States (E-USA; 32–43°N,95–71°W), western United States (W-USA; 32–43°N, 125–100°W), Europe (35–60°N, -10ºW–30°E), central Africa (C-Africa; 4°S-5ºN, 10° – 40°E), northern Africa (N-Africa; 5–15°N, 10°W–30°E), southern Africa (S-Africa; 5–15°S, 10–30°E), South America (S-America; 20°S – 0°N, 50–70° W), India (7.5–35°N, 68–89°E), the Indo Gangetic Plain (IGP; 21–33°N, 72–89°E), (k) east India (E-India; 15–25°N, 80–90°E)), south India (S-India; 0–15°N, 63–80°E), Southeast Asia (SE-Asia, 10–20°N, 96–105°E), and the remote Pacific region (28°S – 32°N, 117°–177°W)

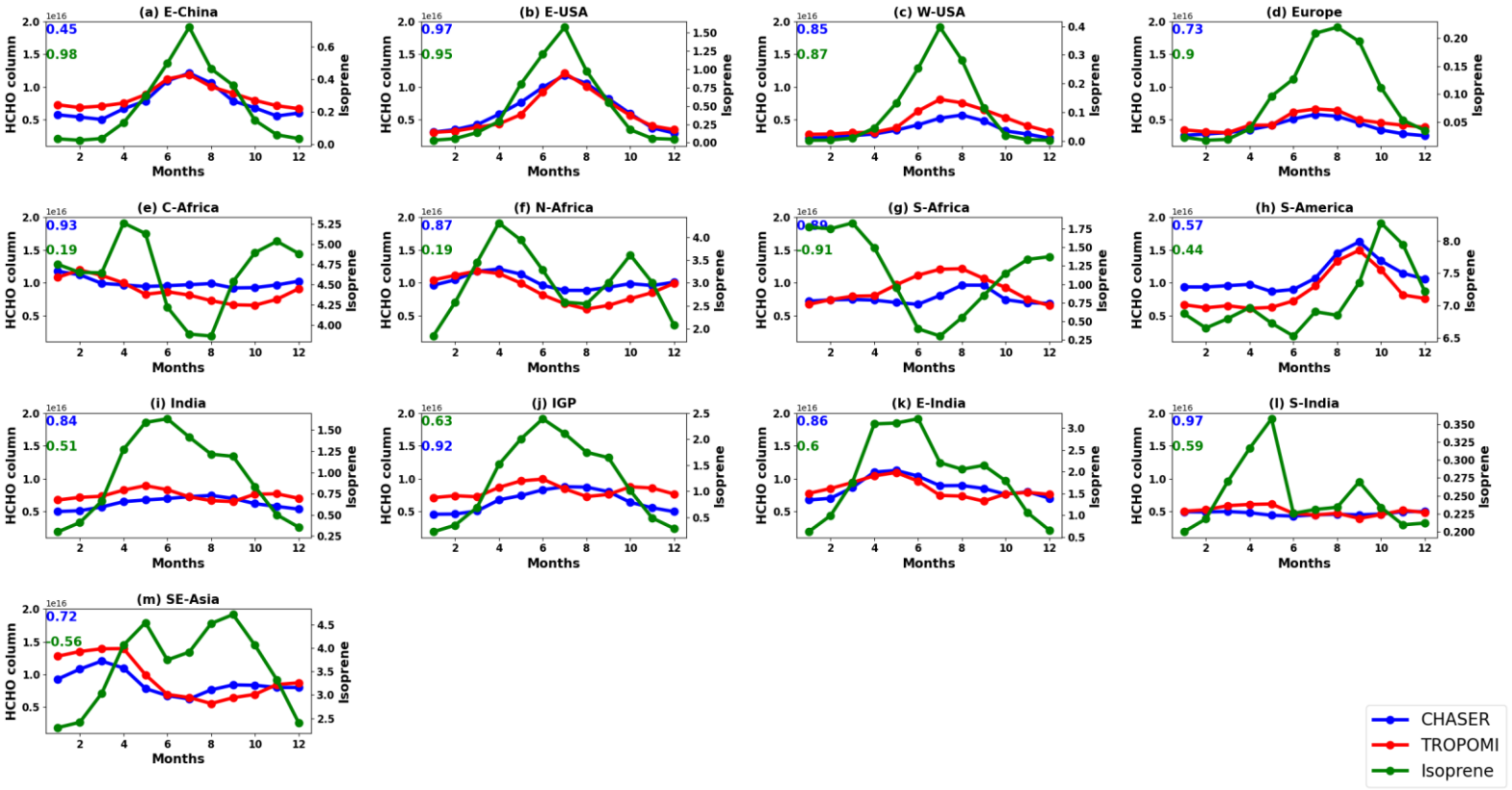

Figure S4. Seasonal variation in HCHO columns (× 10^{16} molecules cm^{-2}) in(a) China (E-China; 30–40°N, 110–123°E), (b) eastern United States (E-USA; 32–43°N,95–71°W), (c) western United States (W-USA; 32–43°N, 125–100°W), (d) Europe (35–60°N, -10ºW–30°E), (e) central Africa (C-Africa; 4°S-5ºN, 10° – 40°E), (f) northern Africa (N-Africa; 5–15°N, 10°W–30°E), (g) southern Africa (S-Africa; 5–15°S, 10–30°E), (h) South America (S-America; 20°S – 0°N, 50–70° W), (i) India (7.5–35°N, 68–89°E), (j) the Indo Gangetic Plain (IGP; 21–33°N, 72–89°E), (k) east India (E-India; 15–25°N, 80–90°E)), (l) south India (S-India; 0–15°N, 63–80°E), (m) Southeast Asia (SE-Asia, 10–20°N, 96–105°E), and (n) the remote Pacific region (28°S – 32°N, 117°–177°W) The red, blue, and red lines are TROPOMI retrievals and CHASER simulations, respectively. The green curves signify the simulated isoprene seasonality in the respective regions. The blue number indicates the correlation between TROPOMI and CHASER HCHO columns, whereas the green number is the correlation between TROPOMI retrievals and isoprene concentrations. The unit of isoprene concentrations is ppbv.

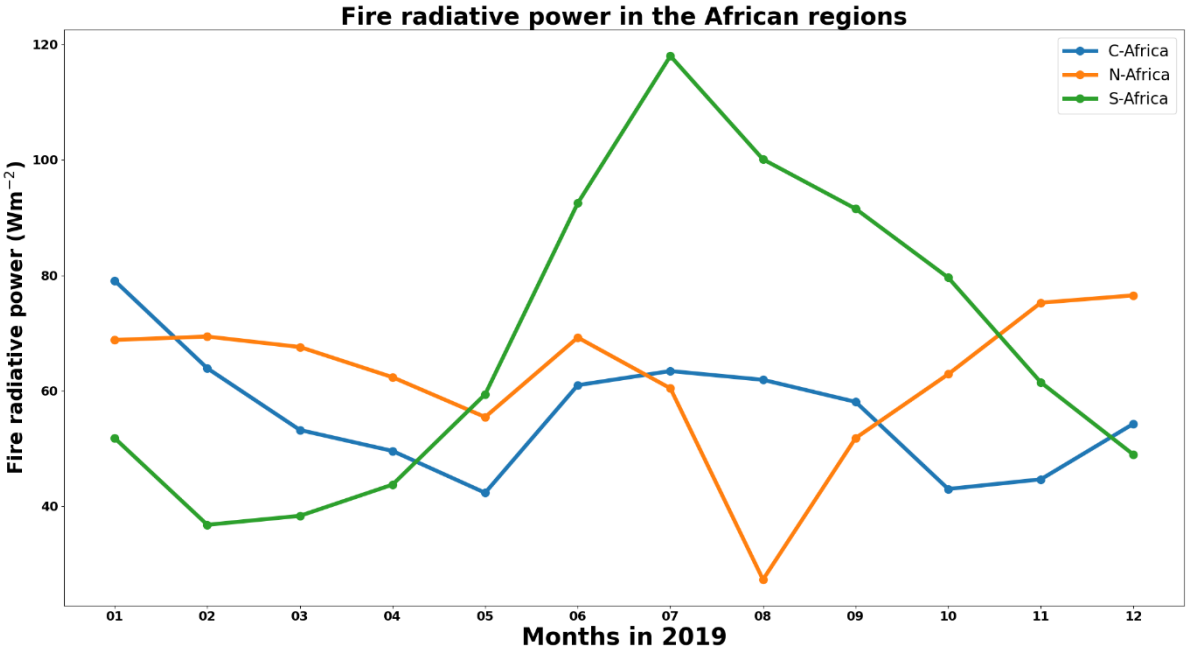

Figure S5. Monthly variations of fire radiative power (blue) and fire numbers (black curve) in the North African region. The fire data are extracted from the MODIS Active Fire Detections database (https://firms.modaps.eosdis.nasa.gov, last accessed on 2022/4/15). FRP retrieval confidence higher than 80% is plotted only.

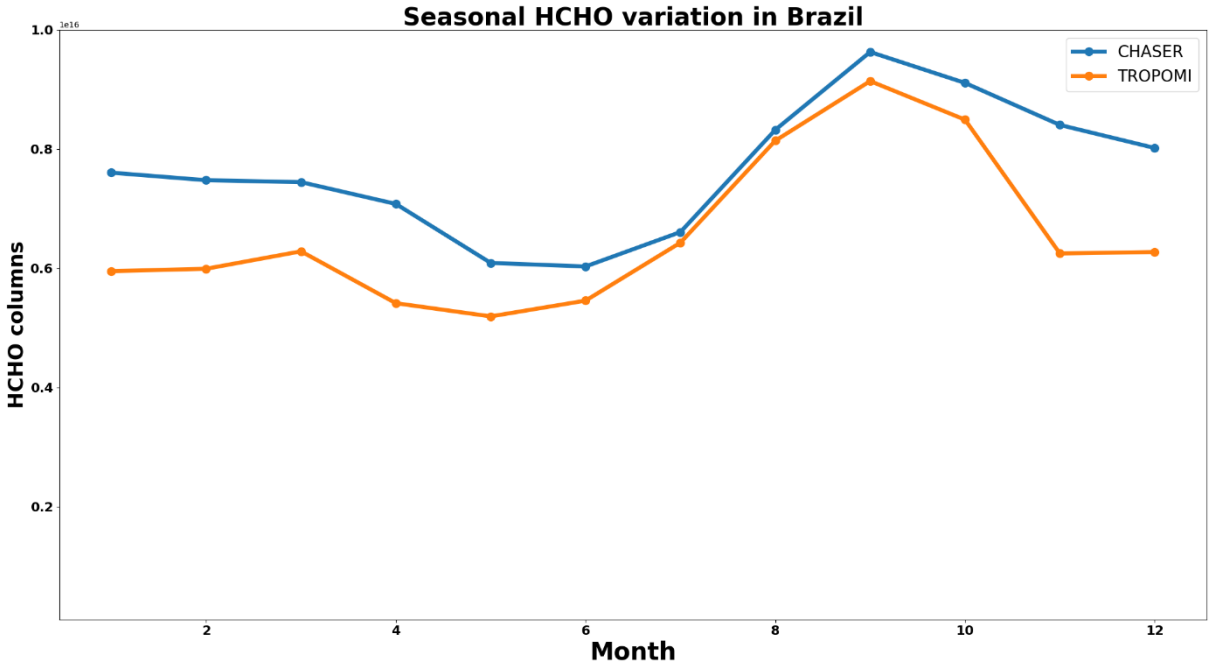

Figure S6. The observed and simulated seasonal variations in the HCHO columns in Brazil. The mean values represent the averages over two years. Only the coincident observations were used to calculate the monthly mean values.

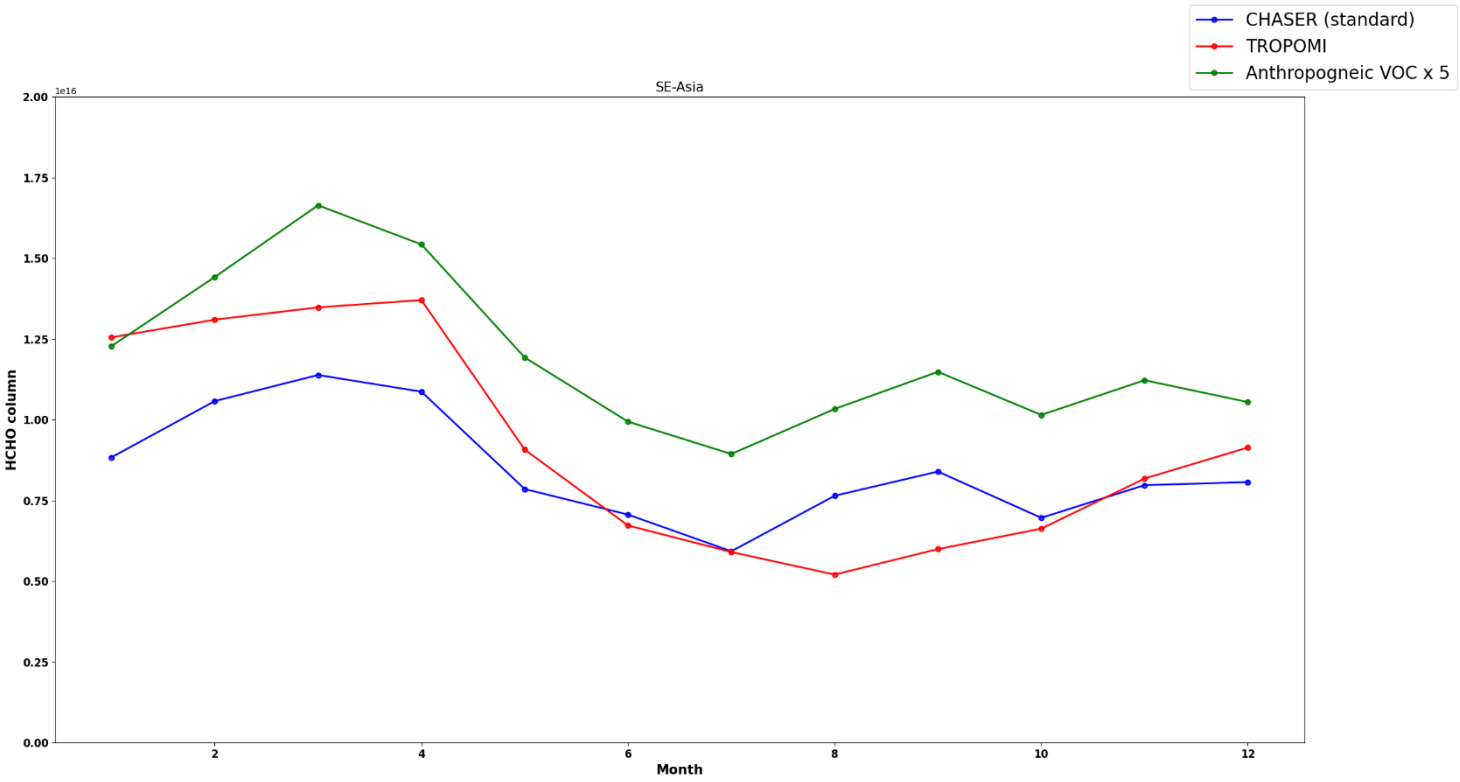

Figure S7. Seasonal variation of HCHO (x 10^{16} molecules cm^{-2}) in Southeast Asia, inferred from standard simulations (blue), TROPOMI observations (red), and ANI estimate (green). Anthropogenic VOC emissions are increased by fivefold in the ANI simulations. The coordinate bounds of Southeast Asia are similar to Fig. 2. The simulation setting is given in Table 1.

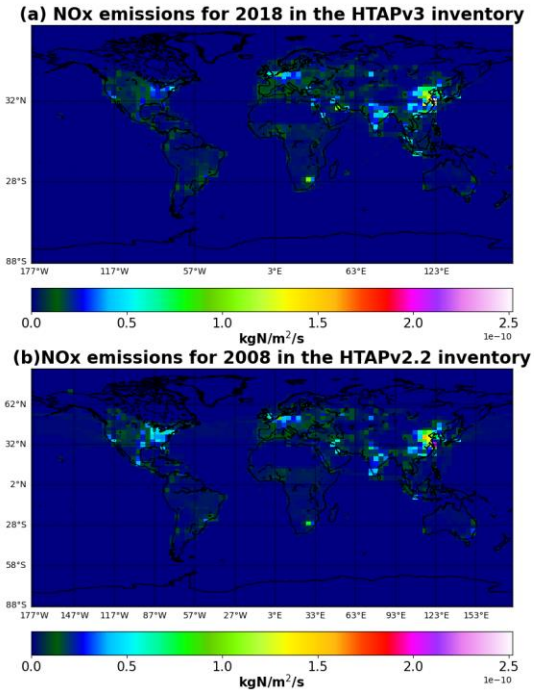

Figure S8. NO_x emissions in (a) HTAPv3 and (b) HTAPv2.2 inventory. The HTAPv3 inventory was used in the standard simulation, whereas the HTAPv2.2 emission inventory was used for the OLNE simulations.

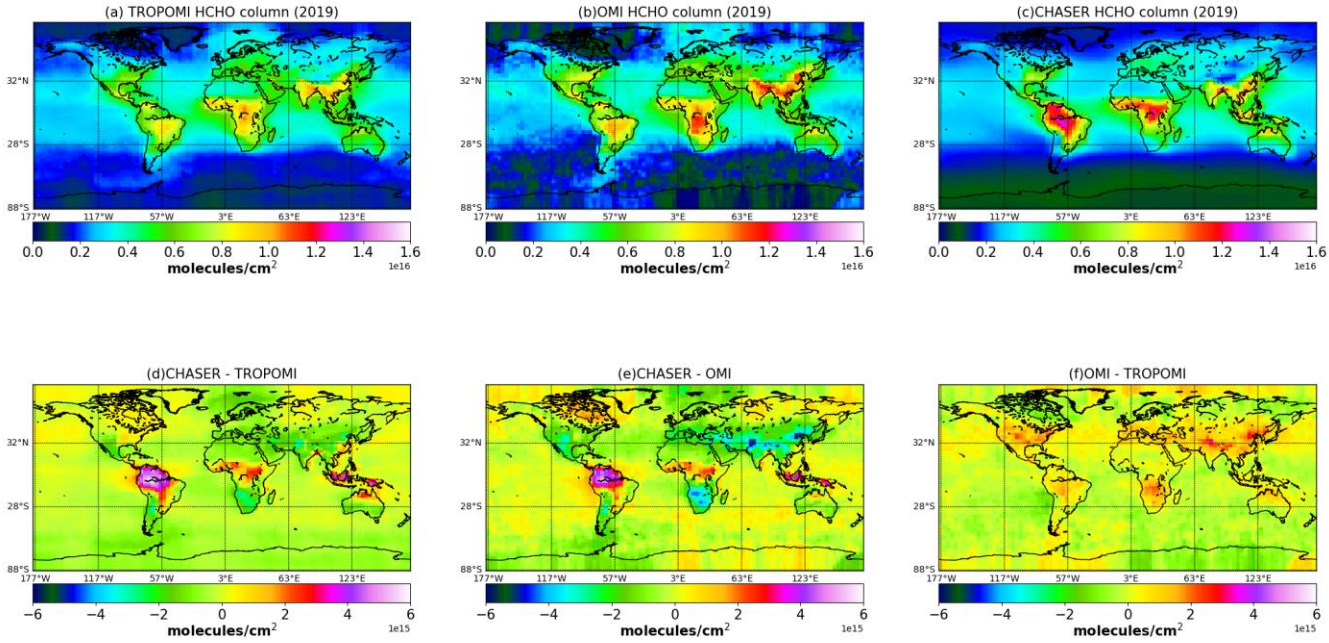

Figure S9. Annual (2019) mean HCHO columns (× 10^{16} molecules cm^{-2}) inferred from (a) TROPOMI and (b) OMI retrievals and (c) standard CHASER simulations. The differences between the two observational datasets are also plotted. The unit of difference is x 10^{15} molecules cm^{-2}.

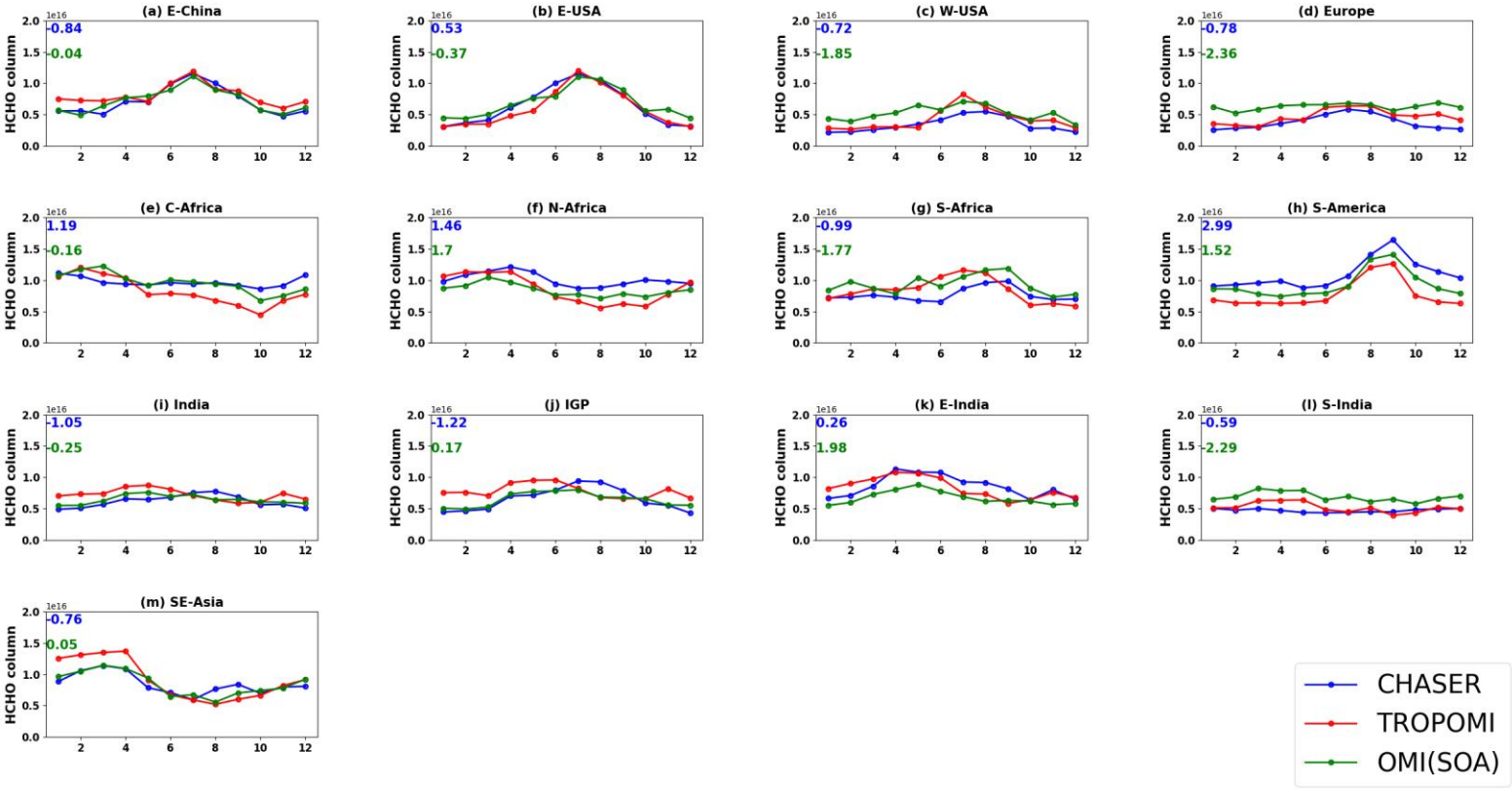

Figure S10: Seasonal variation of HCHO ($\times 10^{16}$ molecules cm^{-2}) inferred from TROPOMI (red curve) and OMI SOA (green curve) retrievals and standard CHASER (blue curves) simulations. The definition of the regions is the same as Fig.2. The blue numbers signify the MBE between TROPOMI and CHASER, whereas the green numbers are the MBE between CHASER and OMI SOA. Coincident dates among the datasets are used to calculate the monthly mean data.

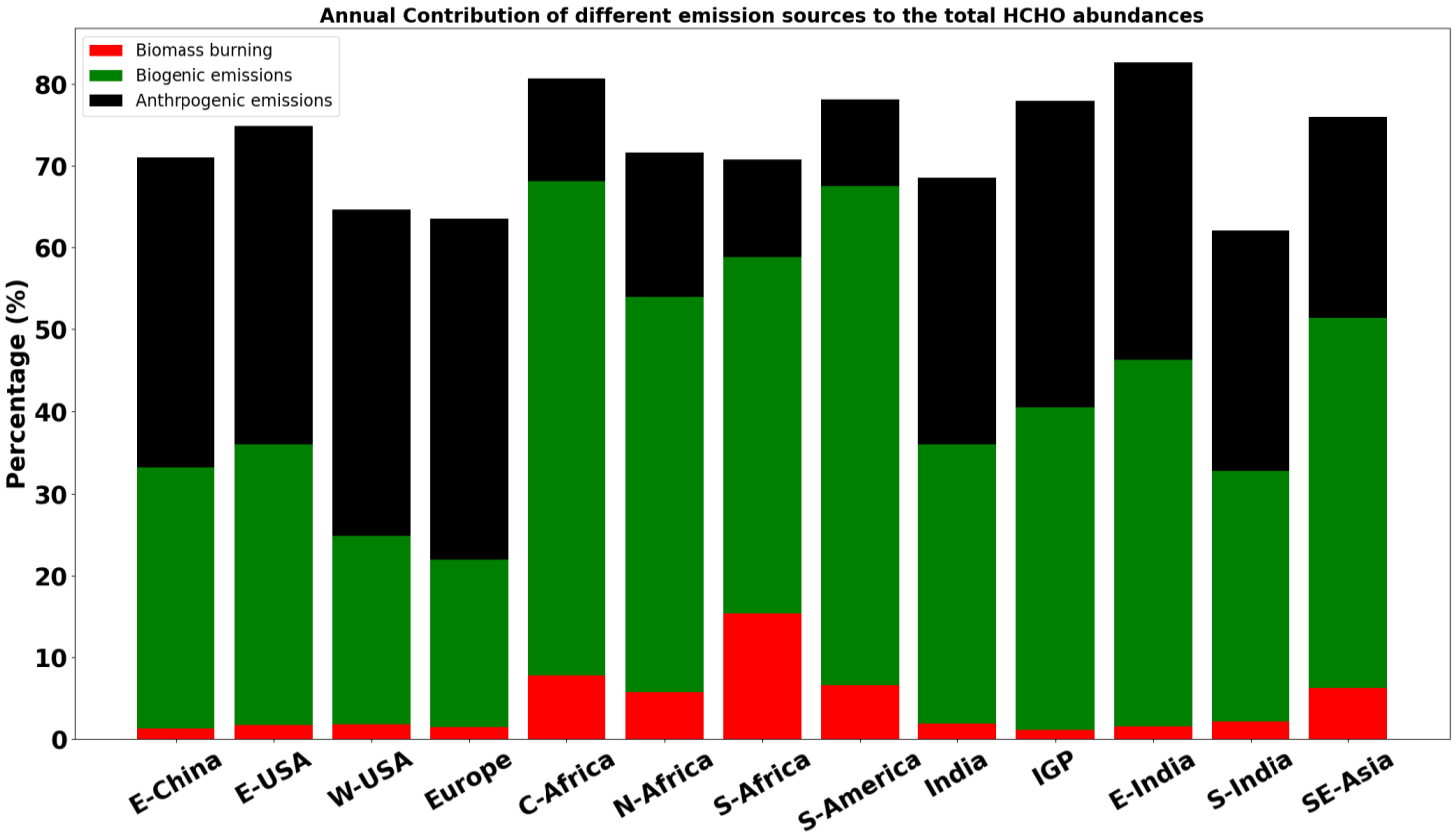

Figure S11: Annual relative contribution (%) of anthropogenic, pyrogenic, and biogenic emissions to the total HCHO column in the selected regions.

Table S1. Statistics of comparison between regional mean tropospheric HCHO simulations obtained from the standard and high-resolution simulations. Units of MBE (standard simulation – high resolution simulations) and RMSE (standard simulation – high resolution simulations) are $\times 10^{16}$ molecules cm^{-2}.

Region	**MBE**	**RMSE**
E-China	-0.13	0.18
E – USA	-0.01	0.04
W-USA	0.02	0.03
Europe	-0.01	0.01
C-Africa	-0.14	0.16
N-Africa	0.08	0.15
S-Africa	0.02	0.13
S-America	-0.06	0.23
India	-0.12	0.13
IGP	-0.27	0.28
S-India	-0.29	0.30
E-India	-0.07	0.08
SE-Asia	-0.02	0.14

Table S2. The temporal correlation between the simulated and observed HCHO columns in different regions. The temporal correlations are calculated from two years of simulated and observed daily mean HCHO abundances.

Region	**Temporal correlation calculated from daily mean values**
E-China	0.63
E – USA	0.85
W-USA	0.74
Europe	0.80
C-Africa	0.51
N-Africa	0.65
S-Africa	0.39
S-America	0.82
India	0.21
IGP	0.33
S-India	0.51
E-India	0.29
SE-Asia	0.72
Remote Pacific	0.30

Table S3: Statistical comparison among regional mean tropospheric HCHO (× 10^{16} molecules cm^{-2}) columns inferred from TROPOMI observations, standard simulation, and OLNE estimates. Units of MBE1, MBE2, RMSE1, and RMSE2 are × 10^{15} molecules cm^{-2}.

Region	MBE1 (Standard–TROPOMI)	MBE2 (OLNE–TROPOMI)	RMSE1 (Standard–TROPOMI)	RMSE2 (OLNE–TROPOMI)
Global	-0.23	-0.22	0.75	0.81
E-China	-0.84	-0.24	1.40	1.24
E-USA	0.53	0.39	0.58	0.44
W-USA	-0.72	-0.82	0.80	0.89
Europe	-0.78	-0.86	0.92	0.98
C-Africa	1.19	1.21	1.57	1.57
N-Africa	1.46	1.52	1.61	1.69
S-Africa	-0.99	-1.03	1.32	1.34
S-America	2.99	3.05	3.41	3.45
India	-1.05	-0.58	1.57	1.60
IGP	-1.22	-0.57	1.69	1.67
E-India	0.26	1.01	1.22	1.89
S-India	-0.59	-0.44	0.69	0.62
SE-Asia	-0.76	-0.32	1.16	1.21

Table S4. Monthly MBE and RMSE between satellite observations (TROPOMI and OMI) and CHASER simulations in 2019. Units of MBE and RMSE are $\times 10^{15}$ molecules cm^{-2}. Coincident date and time were used to calculate the statistics.

Month	MBE1 (CHASER – TROPOMI)	MBE2 (CHASER – OMI)	RMSE1 (CHASER – TROPOMI)	RMSE2(CHASER – OMI)
January	-0.17	-0.21	0.99	1.56
February	-0.12	-0.13	0.90	1.60
March	-0.23	-0.42	0.87	1.55
April	-0.25	-0.46	1.08	1.50
May	-0.25	-0.46	1.13	1.63
June	-0.30	-0.54	1.22	1.89
July	-0.28	-0.49	1.30	1.71
August	-0.23	-0.11	1.15	1.48
September	-0.20	0.00	1.21	1.48
October	-0.26	-0.19	1.40	1.92
November	-0.33	-0.02	1.32	1.87
December	-0.20	-0.70	1.21	2.31

Table S5. Comparison of global mean HCHO columns ($\times 10^{16}$ molecules cm^{-2}) obtained from TROPOMI observations, OMI BIRA retrieval, OMI SAO product, and CHASER simulations. Units of MBE and RMSE are $\times 10^{15}$ molecules cm^{-2}.

Region	**MBE1 (Model– TROPOMI)**	**MBE2 (Model - OMI (BIRA))**	**MBE3(Model – OMI (SAO))**	**RMSE1 (Model - TROPOMI)**	**RMSE2 (Model - OMI(BIRA))**	**RMSE3 (Model – OMI(SAO))**
Global	-0.23	-0.24	-1.49	0.77	0.99	1.76
E-China	-0.84	2.54	-0.04	1.40	3.03	1.25
E – USA	0.53	-1.02	-0.37	0.58	1.12	0.64
W-USA	-0.72	-2.09	-1.84	0.80	2.17	1.94
Europe	-0.78	-1.31	- 2.36	0.92	1.60	2.40
C-Africa	1.19	0.94	-0.16	1.57	1.28	1.33
N-Africa	1.45	1.42	1.69	1.61	1.59	1.95
S-Africa	-0.99	-2.59	-1.76	1.32	2.75	2.07
S-America	2.98	2..02	1.52	3.41	2.61	1.80
India	-1.05	-1.91	-0.25	1.57	2.66	1.67
IGP	-1.50	-2.46	0.99	1.56	2.51	1.13
S-India	0.26	0.05	1.97	1.22	1.38	2.54
E-India	-0.69	-0.59	-0.65	0.79	0.71	0.67
SE-Asia	-0.75	-0.83	0.04	1.16	1.14	1.07